Nanotechnology Perceptions
ISSN 1660-6795
www.nano-ntp.com

An Experimental Investigation Into Fluid Flow And Heat Transfer In Rectangular Pin Fin Arrays

S.Balamurugan *[1], R.Karthikeyan[2], R.Muthukumaran[3]

[1]Research Scholar, Department of Mechanical Engineering, Annamalai University*
[2] Professor, Department of Mechanical Engineering, Annamalai University
[3] Assistant professor, Department of Mechanical Engineering, Annamalai University
Corresponding author: er.srbalamurugan@gmail.com

This study focuses on the heat transfer and friction properties of convective heat transfer through a rectangular channel, which includes cylindrical and square cross-section pin-fins attached to a rectangular duralumin flat surface. The pin-fins were set in line and staggered. Different clearance ratios (C/H=0.0, 0.5, and 1.0) and inter-fin distance ratios (Sy/d and Sx/d) were used. The trials are carried out at varied mass flow rates of air (Re ranges from 2000 to 11000). The experimental results demonstrated that using square cross-section pin-fins may provide an advantage in terms of heat transfer enhancement. For better thermal performance, in-line and staggered arrangements should have a lower inter-fin distance ratio and clearance ratio, as well as comparatively lower Reynolds numbers. The findings of the in-line designs were compared to those of the staggered arrangements for the two types of pin-fins.

Keywords: Duct flow, Forced convection, Heat exchangers, Tipclearance, Pin-fin, and pressure drop.

1. Introduction

Thermal management is critical for the semiconductor industry, as the inexorable rise in heat flux densities from microelectronic components and devices presents formidable challenges in keeping processor temperatures below critical values, thereby avoiding a variety of important failure modes, such as chip cracking and thermal oxidation of interconnect surfaces [1]. Because cooling electronics account for around 0.5% of global electricity use [2], innovative cooling methods are necessary that can deal with extremely high heat flux densities over localized hot spots, in excess of 100 W/cm^2, while also lowering energy consumption [3]. These issues have prompted a variety of cooling advances, including the use of highly conductive inserts to provide more effective heat removal paths [4], as well as a number of potential liquid cooling techniques. On-chip cooling, direct liquid jet impingement, and dielectric liquid immersion are some of these methods. They remove heat through convection currents [5], and nanofluids can be used to improve this process [6]. This research focuses on what is now the most popular method for cooling microelectronics due to its low cost,

availability, and reliability: convective heat transfer to air as it flows over a network of extended surface fins on a heat sink [7]. Nagarini et al.'s recent seventy-paper study [8] provides a synopsis of the major advancements in the design of extended surface heat exchangers over the previous two decades. These have clearly established that surface fins are a realistic technique of generating high heat transfer areas while minimizing the main surface area and acting as turbulence promoters, hence increasing heat transfer rates [9]. Heat sinks, fans, and blowers are anticipated to account for more than 80% of electronic thermal management systems, with a market value of more than $14 billion by 2021 [10]. Heat sinks are a low-cost and dependable way to get a large total heat transfer surface area without exceeding the primary surface area, and the surface fins operate as turbulence promoters, increasing heat transfer rates by breaking up the thermal boundary layer. The primary goals of heat sink design are to provide the necessary heat transfer rates, keep processor temperatures below critical ranges, and minimize pressure loss and heat sink mass [8]. A number of studies have investigated the performance of heat sinks with pin fins, known as pinned heat sinks (PHSs) [9]. Some studies, like those by Soodphakdee et al. [11] and Jonsson and Moshfegh [12], looked at the impact of pin cross-sectional shape. Others, like Zhou & Catton [7] and Yang & Peng [13, 14], looked into the benefits of combining plate and pin fins in compound heat sinks. Ashish and Anil's experimental study of the grooved form of a flat fin [14] demonstrated the role of forced convection in revealing heat transfer characteristics. According to the author, the experiment demonstrated grooved fins' ability to improve heat transfer properties over conventional fins. You can modify and alter the fins by incorporating holes, slits, and struts to improve heat transfer; however, we do not strictly recommend the use of ribs or struts. This element of choice increases the bulk or weight of the existing fin, and in such circumstances, using a grooved fin is not recommended owing to material reduction. The literature also reveals that only a limited number of studies have explored the impact of geometrical modifications on heat transfer characteristics, with a focus on grooved fins. Previous research has shown that pin-fin arrays disperse more heat than conventional channels. However, any increase in heat transmission invariably results in a large increase in pressure loss. As a result, in many applications involving pin-fins, both heat transmission and pressure loss characteristics must be considered. This study aims to investigate the heat transfer, pressure, and performance characteristics of in-line and staggered pin-fin arrays (cylinder, grooved cylinder, and perforated cylinder fins) attached to a flat surface in a rectangular channel while accounting for various geometric and flow parameters. The current experimental work examines the impact of heat transfer and fluid flow properties on cylindrical-type fins, comparing their behavior to that of cylinder, grooved cylinders and perforated cylinders. The experiment validates the results as dimensionless geometrical functions of fins.

2. Experimental setup

This chapter discusses the manufacture of pin-fins and the equipment required for wind tunnel experiments. Wind tunnels commonly conduct forced convection tests to assess the performance of heat transfer test modules. Subsequent sections are devoted to discuss these in detail.

2.1 Pin-fin Assembly

The pin-fin arrays used in this study have cylinder, grooved cylinder, and perforated cylinder pin-fins with dimensions of 10 mm diameter and 90 mm height, respectively. As shown in Fig. 2, the pin-fins used in this study include a cylinder with a diameter of 10 mm and a height of 90 mm, a grooved cylinder with a diameter of 8 mm and a height of 3.2 mm, and a perforated cylinder with holes of 4 mm diameter through cylindrical fins at 19.5 mm from the base. The fin extends upwards from a 250 mm x 145 mm rectangular horizontal base with a thickness of 25.4 mm. You can adjust the fin spacing based on the number of fins. The maximum and minimum number of pin-fins used in this investigation are 60 and 18 respectively. The spacing can be altered in streamwise directions, but span-wise spacing is constant. Simply replace the pin-fins with studs made from the same material. The studs' heads can be fitted flush with the top surface of the horizontal base plate. The rectangular base and pin fins were composed of aluminum alloy. For each test, the pin-fin height was kept constant while the clearance between the pin-fin tips and the shroud was varied. In addition, Figure 1 shows sectional elevations of the pin-fin and pin-fin assemblies.

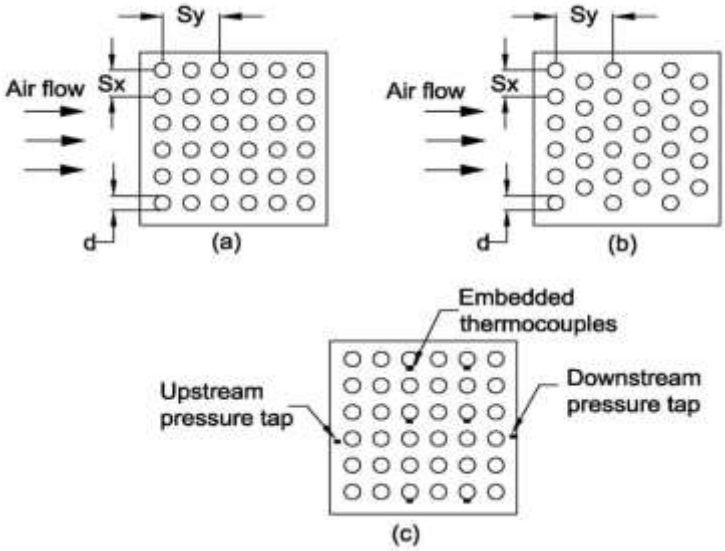

Fig. 1 Arrangement of pin-fin arrays

(a) In-line (b& c) Staggered

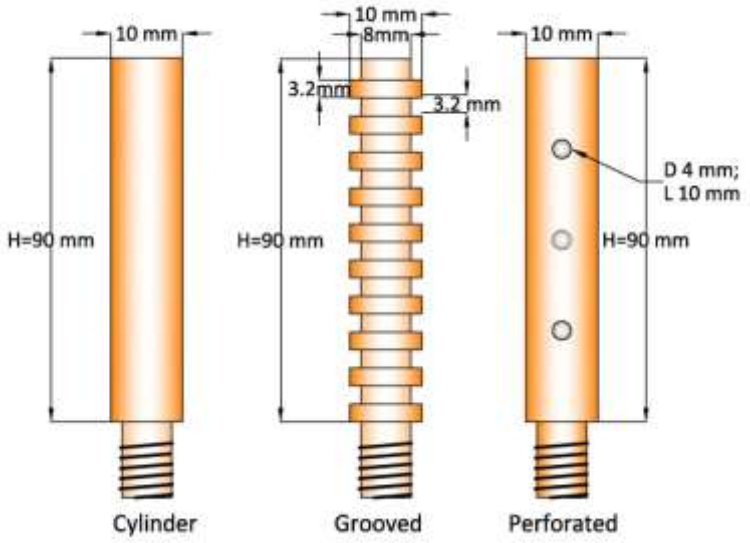

Fig. 2 Pin-fin assembly

2.2 Wind tunnel

The primary body of the wind-tunnel duct was made of 19 mm thick plywood with a constant internal width of 150 mm and a length of 2 meters. Figure 3 depicts the schematic of the experimental setup. The thesis concludes with photographs of the setup. Duct height was adjusted using the movable horizontal roof (or shroud). The duct has a consistent vertical height and a variable cross-sectional area.

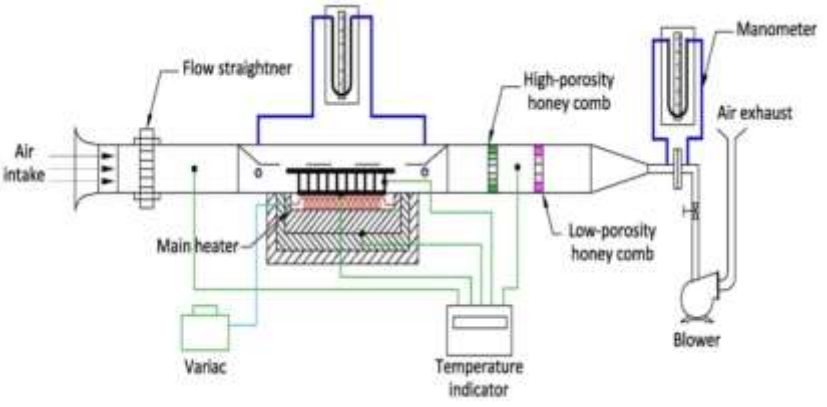

Fig. 3 Experimental setup

The test component was halfway down the duct's length. The wind tunnel's entrance features a bell-mouth section, followed by a low-porosity cardboard honeycomb flow straightener. Two cardboards, one with low porosity and the other with high porosity, form an insulated chamber that mixes the heated air from the fin assembly. A gradual contraction section was employed at the exhaust end to link a single-speed, single-stage blower (via G.I. pipe). The blower has a maximum flow rate of 0.242 kg/s. A butterfly valve precedes it. A differential manometer was utilized to determine the pressure drop across the orifice plate. The blower may draw in ambient air through the bell-mouthed entrance. Air travels through the fin assembly and test portion. This prevented the blower from heating the air stream during compression prior to the heat exchanger assembly, increasing the air's cooling capabilities.

2.3 Experimental procedure

The wind tunnel houses each pin-fin array test module, complete with appropriate instrumentation and sensors. To acquire steady state observations, all tests maintain an average base plate temperature of ~50 ±0.25 ^{o}C. We collected data for six mass flow rates of air: 0.069, 0.089, 0.105, 0.119, 0.132, and 0.143 kg/s. We manually record the temperatures of the input and outflow air, along with the base plate, based on the previously mentioned mass flow rates.

Table 1 Experimental conditions

Parameters	**Minimum value**	**Maximum value**
x-direction pin-fin spacing [S_x] (mm)	24	24
y-direction pin-fin spacing [S_y] (mm)	24	228
Mass flow rate [m] (kg/s)	0.069	0.143
Clearance ratio [C/H]	0.0	1.0
Total number of fins [N_{xy}]	18	60
Reynolds number [Re]	2000	11000
Diameter of cylindrical pin-fin [d] (mm)	10	
Height of cylindrical pin-fin [H] (mm)	90	
Base plate W x L (mm)	145 x 250	
Diameter of Groove (mm)	8	

Height of grooved (mm)	3.2	
Perforation hole diameter (mm)	4	
Base plate temperature [t_b] (^oC)	~50 ±0.25	

3. Data reduction:

It calculates the friction factor and heat transfer based on the measured data. The steady-state heat transfer for the finned surface is calculated as follows:

$$Q_{tot} = Q_{conv} + Q_{rad} + Q_{loss} \quad (1)$$

Below is the entire steady-state energy equation for the system: The data reduction adopted in this case is comparable to that of Naik et al. (21), Jubran et al. (16), and Tahat et al. (18). They conducted testing and discovered that fin arrays are equivalent, with less than 5% heat loss capacities. Equation (1) is presented even though, given the current operating conditions, the insulation of the test portion, and the assumption that the loss is very minor.

$$Q_{conv} = m\, c_p(t_{out} - t_{in}) \quad (2)$$

The base plate and convective heat transfer fin surface are provided by

$$Q_{conv} = h\, A_s \left[t_b - \left(\frac{t_{in} + t_{out}}{2}\right)\right] \quad (3)$$

Where are the air flow temperatures, the average temperature at the base assembly's center, and the total test surface area, which can be written as,

$$A_s = WL + \pi\, d\, H\, N_{xy} - \frac{\pi d^2 N_{xy}}{4} \quad (4)$$

Combining the equations yields the average heat transfer coefficient for the heated pin-fin assembly. (2) and (3):

$$h = \frac{m\, c_p(t_{out} - t_{in})}{A_s\left[t_b - \left(\frac{t_{in} + t_{out}}{2}\right)\right]} \quad (5)$$

Given the current operating conditions and the well-insulated test section, the free flow area is calculated as follows:

$$A_{ff} = W(H + C) - N_x\, H\, d \quad (6)$$

The Nusselt number is calculated using the previous heat transfer coefficient value as conventionally,

$$N_u = \frac{h\,D}{k} \tag{7}$$

The Reynolds number (Re) is defined as

$$R_e = \frac{G\,d}{\mu} \tag{8}$$

3. Results and discussions

The numerous heat transfer-related characteristics described above are utilized to analyze the influence of pin-fin with a pin-fin area of approximately 8% of the base plate used in the study. Separately or jointly, the acquired results for distinct parametric influences on heat transmission are examined.Pin-fin spacing, Clearance ratio,Pin-fin area (number of fins), Pin-fin shape (cross-section) and Pin-fin array.

3.1 Effect of pin-fin spacing

Heat transfer measurements were carried out with a constant Sx=24 mm and Sy=24 to 228 mm, with three C/H values of 0.0, 0.5, and 1.0. Each sample included data at six distinct mass flow rates: 0.069, 0.089, 0.105, 0.119, 0.132, and 0.143 kg/s. The Reynolds number used in the experiment ranged between 2000 and 12000. The graph in Figure 1 shows the relationship between the Nusselt number and the stream-wise spacing ratio (Sy/d) for solid, perforated, and cylindrical pin fin arrays with the given C/H and air mass flow rates, as well as for the in-line arrangement. The figures clearly demonstrate that increasing the mass flow rate and spacing improves the thermal performance of the pin-fin array.

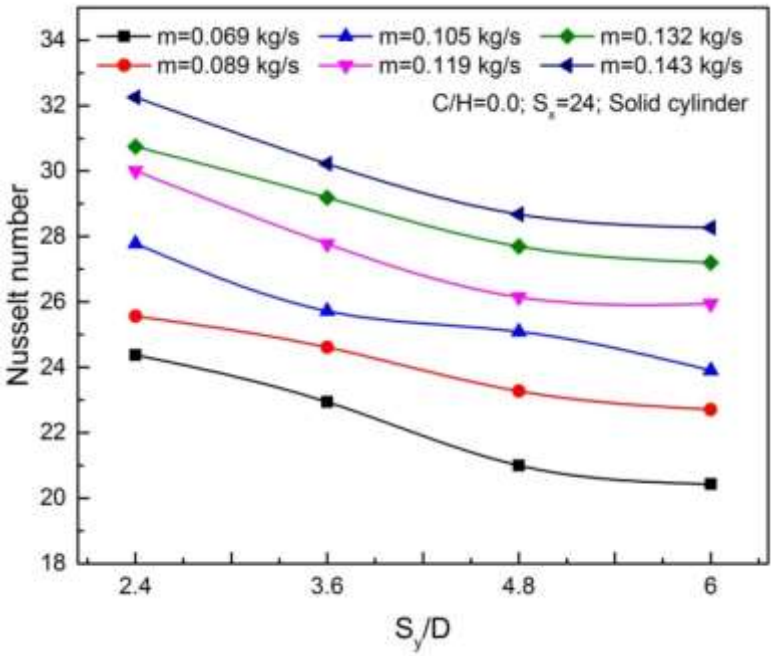

Fig. 4 Plot of Nusselt number VsS_y/d for C/H=0.0, S_x= 24 (Solid cylinder)

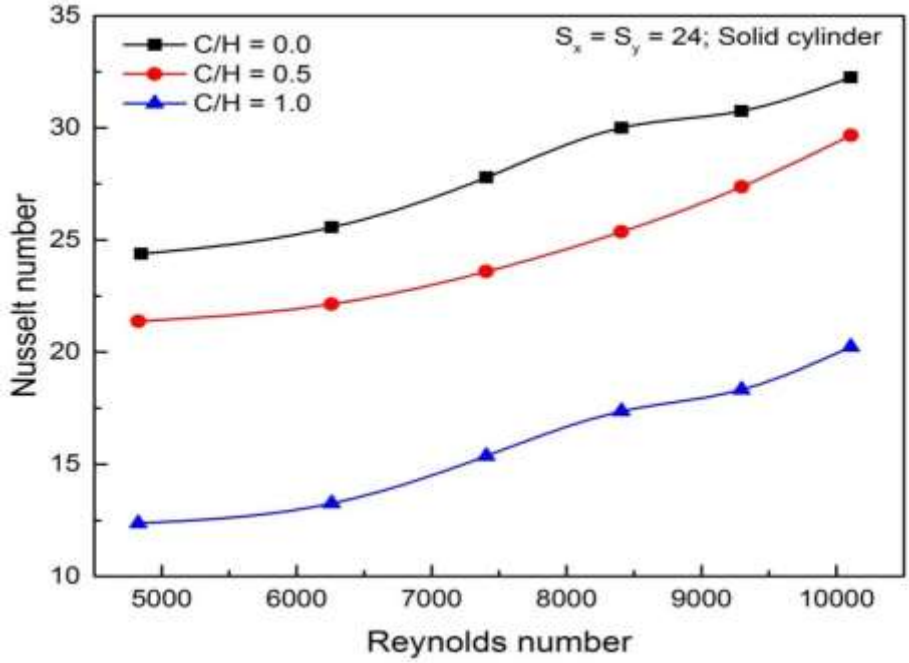

Fig. 5 Plot of Nusselt number VsS_y/d forC/H=0.0, S_x=S_y=24 (Solid cylinder)

3.2 Effect of clearance ratio (C/H)

Figure 5.6 shows the influence of clearance ratio on heat transfer rate over the Reynolds number range covered by the studies. For all C/H values, the heat transfer rate appears to increase monotonically with Reynolds number. Furthermore, increasing the spatial compactness of the heat exchanger results in the highest heat transfer at the smallest C/H ratio. Previous researchers have reported on this strategy (Jubranet et al., 16; Tahatet et al., 17; Tahatet et al., 18;;Kadiret et al., 2001; Sara, 20). The highest heat transfer occurs at smaller inter-fin distances in both the span-wise and stream-wise directions; however, the pressure drop across the pin-fin array was such that the fins impeded the flow.

3.3 Effect of pin-fin surface area / number of fins

Typically, the array reduces the inter-fin distance to improve heat transmission. Figure 6 illustrates the effect of surface area on pin-fin performance in a cylindrical pin fin array. Including an appropriate number of pin-fins in the array (packing density Nxy/Ab) modifies the surface area. The largest surface area from the fewest number of fins improves performance at the expense of pumping power, but not thermally. Because the pin-fin surface area is large, especially for lower Sy/d values, the fluid flows in a stream-wise direction with less influence. This is because the pin fins beyond the first row of an array are in the turbulent wake of the upstream pin fins. For modest values of Sy, the turbulence of the flow enhances the convection coefficients associated with downstream rows. However, with tiny values of Sy, the upstream rows effectively shelter downstream rows (wake effect), reducing the rate of heat transfer. The preferred flow path is in lanes between the pin fins, which protects much of the pinfin surface area from the main flow. Fig. 6, which plots Nusselt's number against spacing, observes a similar effect in geometrically modified (perforated) pin fins.

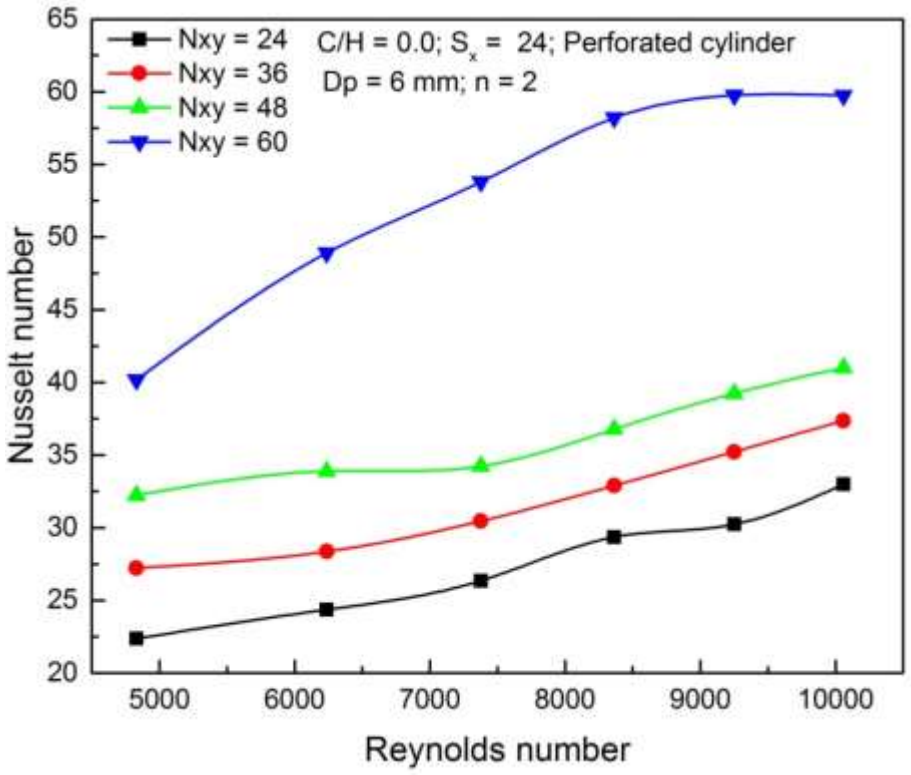

Fig. 6 Plot of Nu Vs Reynolds number for C/H=0.0, Sx= 24 (Perforated cylinder)

3.4 Effect of pin-fin shape and array

In a pin-fin array, turbulence (flow reattachment or delay separation) improves heat transfer. Figures 7 illustrate how the pin-fin profile shape (cylinder, grooved cylinder, and perforated cylinder) affects heat transfer augmentation. Despite the fact that four pin-fin profiles have a distinct surface area, grooved cylinder fins outperform cylinder, square, and perforated cylinders, as well as perforated squares. The staggered pin-fin arrays perform better than the other configurations. Beyond the first row of pin-fins, the wake flow effect is less pronounced. The free flow fluid/air between any two adjacent pin-fins of the upstream row flows over the succeeding downstream rows, resulting in additional boundary layer formation that increases heat transport. In a staggered array, the main flow course is more tortuous/convoluted.

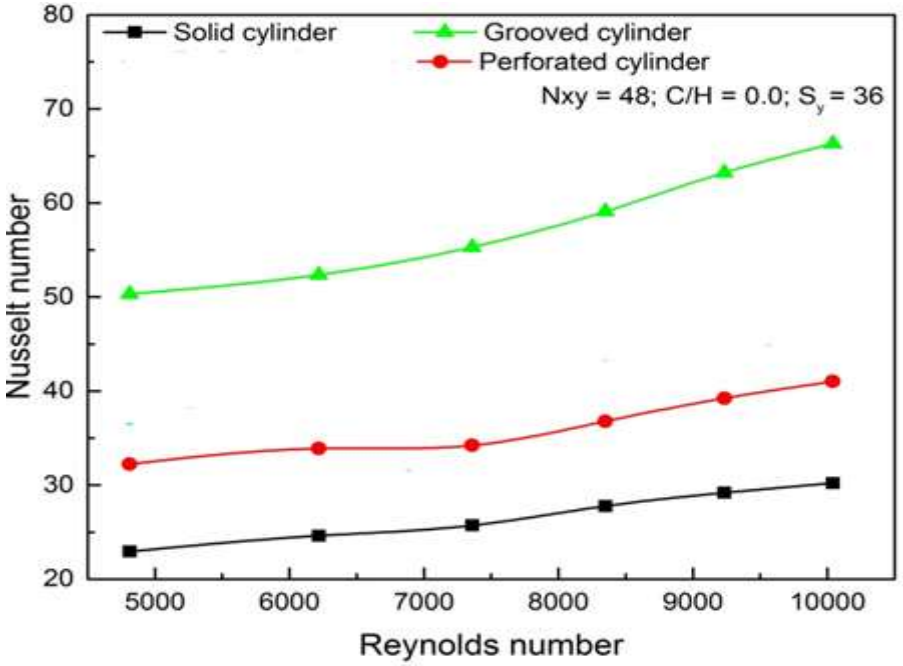

Fig. 7 Effect of pin-fin-shape on Nu for C/H=0, S_x= 24, S_y= 36

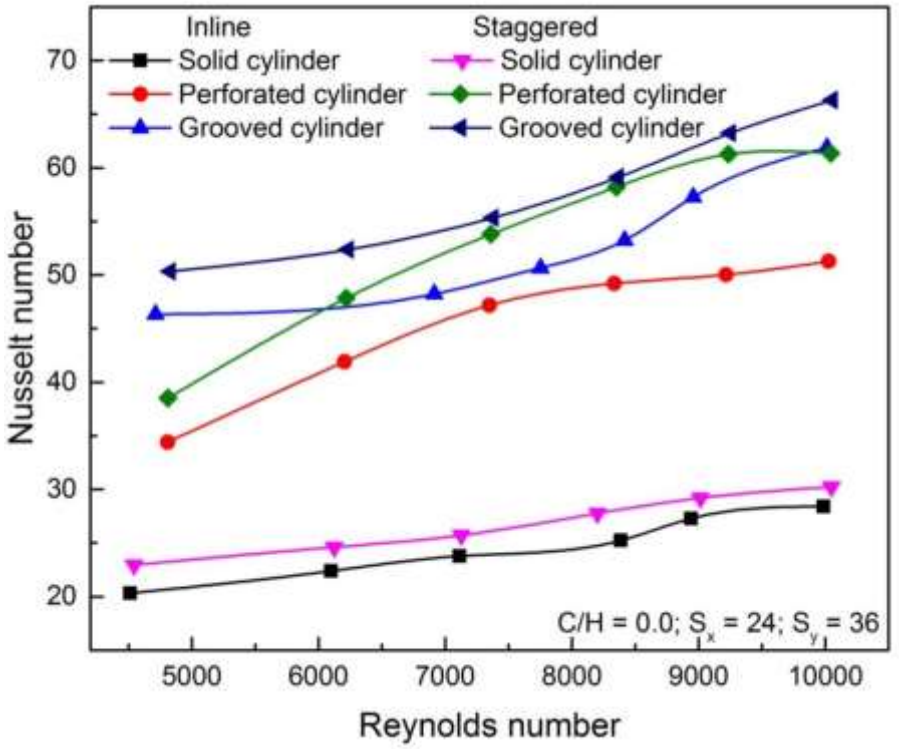

Fig. 8 Effectof Pin-fin Perforation Location

Many members of the heat transfer research community attempt to improve heat transfer (Sara et al., 2000) in pin-fin arrays using a variety of strategies. One of these is perforation. Figure 9 shows how hole placement affects the fin's thermal performance. To investigate the perforation positions, three configurations are considered to investigate the positions of perforation, which are 22.5 mm, 45 mm, and 67.5 mm from the base. Among these arrays, the pin-fin array with perforation 45 mm from the base had a higher rate of heat transmission than the other locations (22.5 mm and 67.5 mm). This shows or explains why holes in the fins that are 45 mm apart cause faster convection. The holes in the middle position also change the flow in the wake region, which causes main flow to hit the downstream pin-fin. In other words, the flow through the perforations at that location not only enhances turbulence but also regulates flow separation in contrast to others.

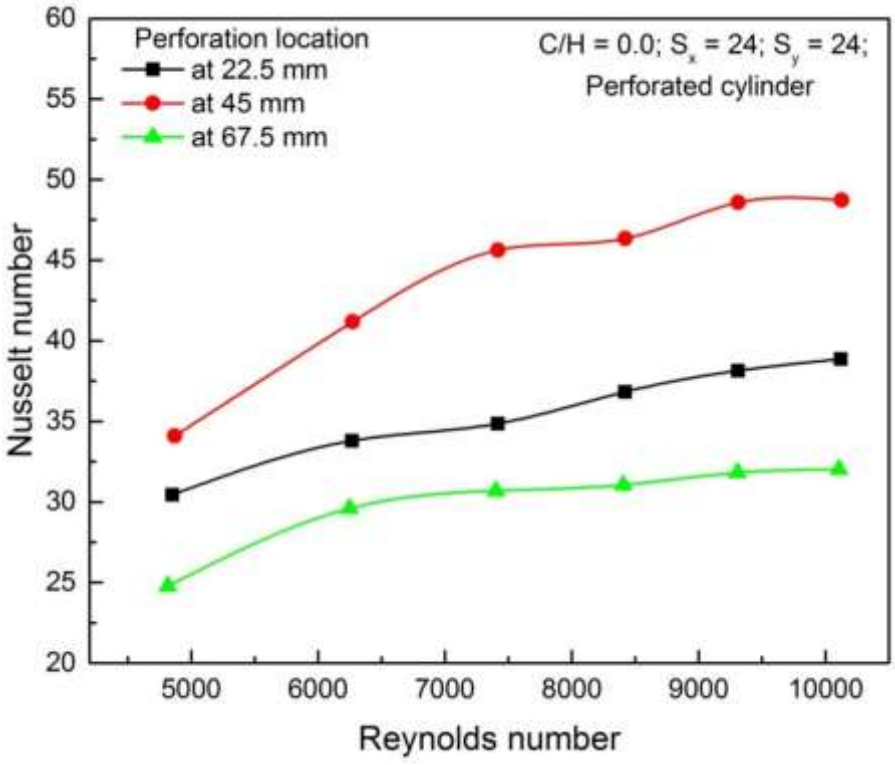

Fig. 9Effect of NurVs Re for C/H=0.0; S_x= 24; S_y=24. (Perforated cylinder)

3.5 Effect of perforation diameter & number of perforation on pin fin

The pin fin's design and dimensions limit the number and diameter of perforations that can be employed. Thus, it is critical to investigate the relative contribution of these effects to thermal performance on a pin fin array with the same surface area. It is depicted in Figure 10. Researchers have discovered that an increase in the diameter of the perforation leads to an increase in the Nusselt number. As the number of perforations increases, the heat transfer surface contact area increases. Perforated pin fin heat sinks provide significantly greater thermal dissipation compared to solid pin fins. More crucially, thermal dissipation is greater with a larger number of perforations on pin fins than with solid pins for a given perforation diameter. We find that the diameter of each pin fin's perforation increases the nusselt number and Reynolds number. Figure 10 demonstrates that increasing the hole diameter from 2 to 4 mm increases Nu. However, increasing the hole diameter from 4 to 6 mm decreases Nu. This is because a larger number of perforations may reduce the obstruction effect on the flow, resulting in smaller but larger wakes behind the pins. Another factor is a decrease in the cross-sectional area of the pin for heat conduction along the pins.

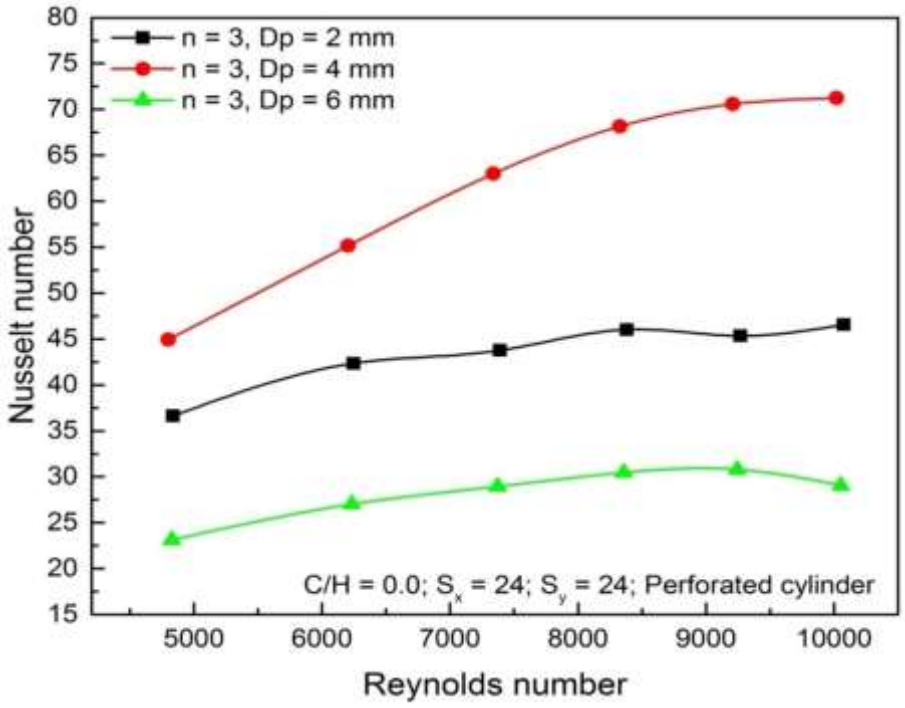

Fig. 10 Effect of Nu Vs Re for C/H=0.0; S_x= 24; S_y=24.(Perforated cylinder)

3.6 Comparison with other heat transfer correlations

It is customary to present heat transfer data in terms of Nusselt number variation against Reynolds number. For the present work one such plot is given in Fig. 11. It is clear that the Nusselt number arrived at are increasing with Reynolds number. In order to validate the data previous work are being compared. The present results are closer to and higher than the result of Kadiret al, (19) and much lesser than the results of Jubranet al, (16) and Tahatet al, (18) with in the range of experimental conditions.

$$Nu = 0.45(Re)^{0.71}\left(\frac{S_x}{W}\right)^{0.40}\left(\frac{S_y}{L}\right)^{0.51} \qquad \text{in - line} \qquad (1)$$

$$Nu = 9.02x10^{-3} Re^{1.011} \left(\frac{S_x}{W}\right)^{0.285} \left(\frac{S_y}{L}\right)^{0.212} \quad \text{in - line} \qquad (2)$$

□□□□□□

$$Nu = 0.2721 \ (Re)^{0.46} \frac{(S_y)^{0.17}}{(L)} \quad \text{in - line} \qquad (3)$$

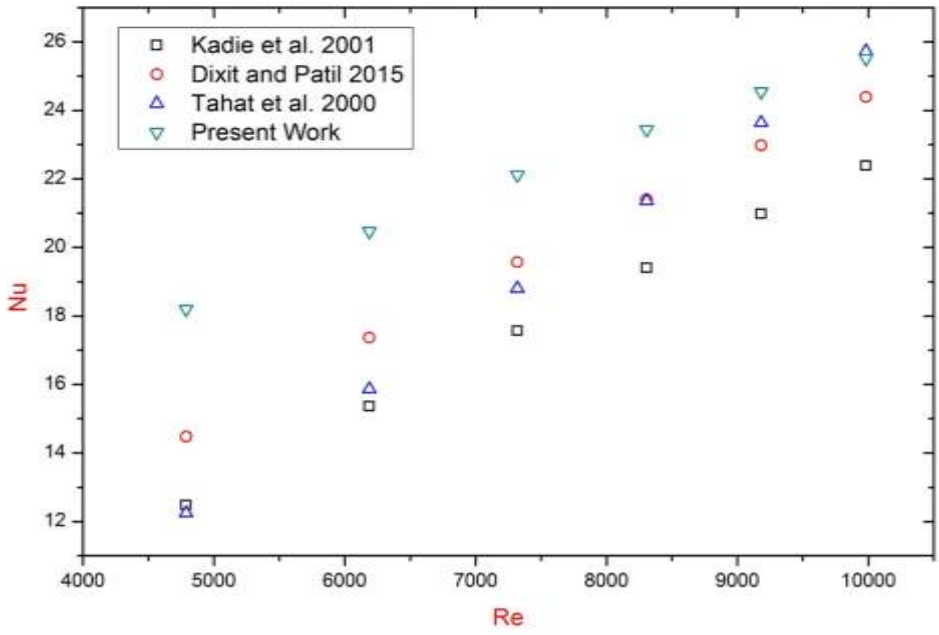

Fig. 11 Plot of Nusselt number vs Reynolds number (with other correlation)

3.7 Heat Transfer Correlations

Figure 12 illustrates how the Nusselt number fluctuates with the Reynolds number for an in-line and staggered array of cylinders with typical Sx and Sy values. The data reveals a clear change from one number to the next, which is dependent on specific variations in Sx and Sy, as well as the pin-fin array. The figure shows that the Nusselt number and Reynolds number are non-dimensional and therefore insufficient to capture the experimental data. Furthermore, it is obvious that additional correlations do not suit the current data (Fig. 5.19). As anticipated, a correlation between the Reynolds number and the pin-fin space distribution data is necessary. Therefore, we fit the current data to a relation of the following form:

$$Nu = C_1 (Re)^b (S_x / W)^c (S_y / L)^d \quad (4)$$

as

$$Nu = 0.42 (Re)^{0.47} (S_x / W)^{0.01} (S_y / L)^{0.01} \quad (5)$$

for in-line arrangement of cylindrical pin-fin array and The diagram illustrates the staggered layout of a cylindrical pin-fin array. Fig. 12 displays equations (4) and (5) along with experimental data. We derive an overall uncertainty of approximately 14% for the above empirical connection.

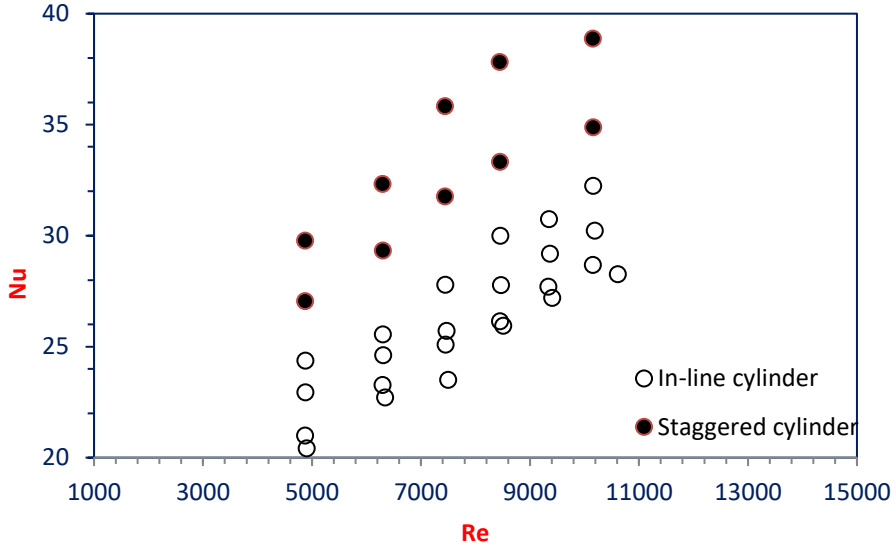

Fig. 12 Plot of Nusselt number Vs Reynolds number (experimental)

4. Conclusions

The heat transfer properties of fin-pin assemblies were tested experimentally in a wind tunnel. The current study's results are summarized. Both span-wise and stream-wise direction spacing affect the Nusselt number. This effect is more noticeable in the streamwise direction. The Nusselt number varies faster in the stream-wise direction (Sy) than in the span-wise direction. Regardless of array architecture, the Nusselt number has a maximum value for a specific packing density or number of pin-fins. In both in-line and staggered arrangements, the average Nusselt number grows monotonically as the Reynolds number rises. The average Nusselt number went up steadily as the clearance ratio went down. However, the inter-fin distance ratio had a non-monotonic effect on the Nusselt number in both in-line and staggered arrangements. For the greatest Qpp, there is an optimal inter-fin distance ratio (or spacing).

For a given Reynolds number, the pin-fin array with a particular interfin distance or number of pin-fins outperforms those with other values. When compared to those without perforations, perforated pin-fins improve heat transfer. Furthermore, the position of perforations influences heat transfer.

Appendix : Notations used this manuscript

A	–	area, (m^2)
C	–	vertical clearance between fin tip and shroud (m)
C_1	–	constant (Nusselt number correlation coefficient)
c_p	–	specific heat of air at atmospheric pressure, (J/kg K)
d	–	pin-fin diameter, (m)
D_e	–	hydraulic diameter (m)
f	–	friction factor
G	–	mass flux [= m/A_{ff}], (kg/m^2 s)
h	–	heat-transfer coefficient, (W/m^2 K)
H	–	pin-fin height (m)
k	–	thermal conductivity, (W/m K)
L	–	base plate length (m)
m	–	mass flow rate of air, (kg/s)
N	–	number of pin-fins
p	–	static-air pressure, (N/m^2)
pp	–	pumping power (W)
Q	–	steady-state heat transfer rate, (W)
Re	–	Reynolds number [= Gd/μ]
S	–	fin pitch, i.e.; distance between adjacent pin-fins (m)

t	–	temperature, (^oC)
T	–	temperature, (K)
v	–	mean speed of the air in the wind-tunnel duct, (m/s)
W	–	base plate width, (m)
x,y,z	–	set of cartesian coordinates
α	–	aspect ratio [=H/d]
$\rho\Delta$	–	difference
μ	–	dynamic viscosity, ($N{\cdot}s\ {\cdot}m^{-2}$)
ν	–	kinematicviscosity, ($m^2{\cdot}s^{-1}$)
ρ	–	density, ($kg{\cdot}m^{-3}$)

5. References

[1] Gurrum S, Suman S, Joshi Y, and Fedorov A.Thermal issues in next-generation integrated circuits. IEEE Trans Device Mater Reliab 2004;4(4):709e14.
[2] Suresh, Garimella, Tim Persoons, Justin Weibel, and Lian-Tuu Yeh. Technological drivers in data centers and telecom systems: multiscale thermal, electrical, and energy management. Applied Energy 2013; 107, 66e80.
[3] Paolo Gargini, Francisco Balestra, and Yoshihiro Hayashi. Roadmapping of Nanoelectronics for the New Electronics Industry 2022, 12(1), 308; https://doi.org/10.3390/app12010308
[4] Hajmohammadi M, Alizadeh Abianeh V, Moezzinajafabadi M, and Daneshi M. Fork-shaped, highly conductive pathways for maximum cooling in a heat-generating piece. ApplThermEng 2013;61(2):228e35.
[5] Hopton P, Summers J. Enclosed liquid natural convection as a means of transferring heat from microelectronics to cold plates. In: Semiconductor thermal measurement and measurement symposium (SEMI-THERM), 2013 29th annual IEEE; 2013. p. 60e4.
[6] Ijam A., Saidur R. "Nanofluid as a coolant for electronic devices" (cooling of electronic devices). ApplThermEng2012;32:76e82.
[7] Zhou F, Catton I. Numerical evaluation of flow and heat transfer in plate-Pin fin heat sinks with various pin cross-sections. Numer Heat Transf Part A Appl 2011;60(2):107e28.
[8] The study was conducted by Nagarani N, Mayilsamy K, Murugesan A, and Kumar G. [8]. The study examines the application of extended surfaces in heat transfer issues. Renew Sustain Energy Rev 2014; 29:604e13.
[9]The study by Al-Damook A, Kapur N, Summers J, and Thompson H was published in [9]. The authors conducted an experimental and computational study on thermal air flows in perforated pin heat sinks. ApplThermEng2015;89:365e76.

[10] Xingcum Colin Tong. Development and Application of Thermal Management Materials. 2010; pp. 527e593.
[11]Behnia, and Copeland . The study conducted a comparison of fin geometries for heat sinks in laminar forced convection, specifically focusing on round elliptical and plate fins in staggered and in-line configurations. Int J Microcircuits Electron Packag2001;24:68e76.
[12] Alok Ranjan, Ranjan Das Himadri Majumder, and Sameer Numerical and Optimization-Based Study on Split Hemispherical Shaped Fins for Augmenting Heat Transfer Rate Hindawi International Journal of Energy Research, 2023 (https://doi.org/10.1155/2023/8300877)
[13] Yang YT, Peng HS investigated the use of planted pin fins to enhance heat transfer in plate fin heat sinks. MicroelectronReliab2009;49:163e9.
[14] Jingshan Yang, Keyong Cheng, Kai Zhang . Conducted a numerical study on the thermal and hydraulic perforances of a hybrid manifold microchannel with bifurcations for electronics cooling. Thermal engineering is applied. 2023; 232, 121099.
[15] Sreya Sarkar, Rohit Gupta, Tamal Roy, and Ranjan Ganguly. Review of jet impingement cooling for electronic devices: International Journal of Heat and Mass Transfer, 2013;206 (23).
[16]. Jubran BA, Hamdan MA, Abdualh RM. The study focused on improving heat transfer, addressing the issue of missing pins, and optimizing cylindrical pin fin arrays. Trans. ASME, Journal. Heat transfer. 1993; 115(3):576e583.
[17] Ming Jeng, Ming Jeng, and Sheng-Chung Tzeng.The researchers conducted a numerical simulation of the laminar forced convection of a pin-fin heat-sink array in a channel using a porous approach. 2015, 5(4), 1846e1868.
[18]. Tahat, M., Kodah, Z.H., Jarrah, B.A., and Probert, S.D, Heat transfer from pin-fin arrays experiencing forced convection, Applied Energy,2000 67, 419e442.
[19]. Kadir, B., Ugur, A., and Sinan, Y. (2001), Heat transfer and friction correlations and thermal performance analysis for a finned surface,Energy Conversion and Management200142,1071e1083.
[20]. Sara, O.N. (2003), Performance analysis of rectangular ducts with staggered square pin fins, Energy Conservation and Management, 44, pp. 1787-1803.
[21] Naik, S., Probert, S.D., and Wood, C.I. (1988), "Thermal hydraulic characteristics of a heat exchanger: The alignment of vertical rectangular fins parallel to the mean air flow in the duct". Applied Energy 29, pp. 217-252.